

# Inverse relationship between D/H fractionation in cyanobacterial lipids and salinity in Christmas Island saline ponds

Dirk Sachse <sup>\*</sup>, Julian P. Sachs

*School of Oceanography, University of Washington, Seattle, WA, USA*

Received 30 August 2007; accepted in revised form 15 November 2007; available online 8 January 2008

## Abstract

Sediments from 28 saline and hypersaline (salinity 13.6–149.2) ponds on Christmas Island (Kiritimati), in the Central tropical Pacific Ocean, were investigated for the effect of salinity on the D/H ratios of lipid biomarkers. Hydrogen isotope ratios (expressed as  $\delta D$  values) of total lipid extracts, and individual hydrocarbons heptadecane, heptadecene, octadecane, octadecene, diploptene, and phytene from cyanobacteria, became increasingly enriched in deuterium as salinity increased, spanning a range of 100‰, while lake water  $\delta D$  values spanned a range of just 12‰. Net D/H fractionation between lipids and source water thus decreased as salinity increased. Isotope fractionation factors ( $\alpha_{\text{lipid-water}}$ ) were strongly correlated with salinity, and increased in all compound classes studied by up to 0.0967 over a salinity range of 136. Differences in the hydrogen isotopic composition of lipids derived from three biosynthetic pathways (acetogenic, mevalonate, and non-mevalonate) remained similar irrespective of the salinity. This suggests that the mechanism responsible for the observed  $\alpha_{\text{lipid-water}}$ –salinity relationship originates prior to the last common biosynthetic branching point, the Calvin Cycle. We propose that a decrease in the exchange of intra- and extra-cellular (ambient) water resulting from down-regulation or closure of water channels (aquaporins) within cyanobacterial cell membranes, and subsequent isotopic enrichment of the intracellular water, likely resulting from metabolic reactions. These findings imply that caution must be exercised when attempting to reconstruct source water  $\delta D$  values using lipid  $\delta D$  values from environments that may have experienced salinity variations. On the other, hand our results can be used to establish a paleosalinity proxy based on lipid  $\delta D$ , if additional constraints on source water  $\delta D$  values can be made.

© 2007 Elsevier Ltd. All rights reserved.

## 1. INTRODUCTION

It has been shown recently, that the stable hydrogen isotopic composition (expressed as  $\delta D$  value, where  $\delta D = (R_{\text{sample}}/R_{\text{standard}}) \times 1000$ ; with  $R$  being the ratio between the abundances of deuterium and protium,  $R = D/H$ ) of a variety of lipid biomarkers can be used to infer the hydrogen isotopic composition of the water used by photosynthetic organisms (Sessions et al., 1999; Sauer et al., 2001; Chikaraishi and Naraoka, 2003; Huang et al.,

2004; Sachse et al., 2004; Englebrecht and Sachs, 2005; Zhang and Sachs, 2007). It has been postulated that the net amount of hydrogen isotopic fractionation between source water and lipids is primarily a function of the biosynthetic pathway, with an as yet unquantified role for environmental factors (Sessions et al., 1999). In terrestrial vascular plants an additional influence on D/H ratios in lipids is the amount of evaporation of leaf water, largely a function of relative humidity and plant physiology (Sachse et al., 2006; Smith and Freeman, 2006). These results have been used to reconstruct changes in the hydrological cycle over various geological timescales (Andersen et al., 2001; Schefuss et al., 2005; Pagani et al., 2006; Pahnke et al., 2007). However, the biological mechanisms and possible responses to environmental conditions that influence the hydrogen isotopic composition of lipid biomarkers remain poorly understood.

<sup>\*</sup> Corresponding author. Present address. Universität Potsdam, Institut für Geowissenschaften, Leibniz Center for Earth Surface and Climate Studies, Karl-Liebknecht-Str. 24–25, 14476 Potsdam, Germany.

E-mail address: [dsachse@geo.uni-potsdam.de](mailto:dsachse@geo.uni-potsdam.de) (D. Sachse).

Recent laboratory studies on algal lipids have found significant differences in net isotopic fractionation between fatty acids from different species of freshwater algae (Zhang and Sachs, 2007). Another study showed that salinity and growth rate, but not temperature, influenced D/H fractionation between source water and alkenones produced by two species of coccolithophorids in batch cultures (Schouten et al., 2006). While the use of species-specific lipid biomarkers can circumvent the problem of variable net D/H fractionation in different species, the influence of salinity on D/H fractionation in lipid biomarkers in the natural environment is unstudied. Further work is also needed on the effects of salinity changes outside the salinity range of 25 to 35 used by Schouten et al. (2006), and in lipids and species other than alkenones from the coccolithophorids *Emiliania huxleyi* and *Gephyrocapsa oceanica*. For these reasons, we targeted the hypersaline lakes on Christmas Island to study the influence of salinity on D/H fractionation in cyanobacteria.

Cyanobacteria are responsible for a substantial fraction of primary production in the ocean today (Lochte and Turley, 1988) and complex microbial communities, organized in microbial mats, are found today in the most extreme environments, such as hypersaline lakes. It is hypothesized that such environments may be analogues for the origin of life on Earth and elsewhere (Simoneit et al., 1998). The widespread occurrence of cyanobacteria makes lipid biomarkers, derived from these photosynthetic organisms, an ideal target for a variety of biogeochemical investigations.

Here, we present an investigation of the hydrogen isotope fractionation between cyanobacterial lipids and environmental water for the three major lipid biosynthetic pathways along a natural salinity gradient of 13.6 to 149.2 in surface sediments and microbial mats from 28 lakes on Christmas Island in the central equatorial Pacific Ocean to evaluate the possibility of using lipid  $\delta D$  values as a proxy for salinity.

## 2. MATERIAL AND METHODS

### 2.1. Sampling sites and methods

Christmas Island is part of the Northern Line Islands in the Republic of Kiribati and lies at 1°52'N and 157°20'W (Fig. 1). It is the world's largest coral atoll with a surface area of 360 km<sup>2</sup> (Valencia, 1977). The island's climate is uniformly dry with a long-term net rainfall minus potential evaporation value of -2 mm/year (Saenger et al., 2006 and references therein). A quarter of the island is covered by hypersaline ponds of various salinities, ranging from the local seawater value (38) up to 150, or higher depending on the year and season. Some ponds are fed by fresh groundwater within the carbonate bedrock and therefore have lower salinities (e.g., lake 168, see Table 1). Temperatures of the lake waters varied between 25.7 and 34.5 °C in June–July 2005. Lake water pH values were between 6.80 and 8.88 (Table 1). A complete description of the physical properties of the lakes sampled on Christmas Island in June–July 2005 is given in Saenger et al. (2006), locations are shown in Fig. 1.

Surface sediments of most of the lakes consisted of gelatinous bacterial mats from a few mm to half a meter in thickness (Fig. 2). The depths of ponds sampled were between 0.19 and 1.71 m (Table 1). For the purpose of this study, surface sediments were divided into bacterial mats (containing several layers of living microbial communities with at least 5 cm total thickness), and surface sediments (containing abundant mineral matter, mostly carbonate debris). The overwhelming sources of organic matter in both types of sediment were cyanobacteria (Trichet et al., 2001), as also revealed by light microscopy (Fig. 2). The upper layers of microbial mats (between 1 and 5 cm) and surface sediments were recovered using an interface coring apparatus that maintained the integrity of the sediment–water interface and left the mat or sediment surface intact (c.f., Fig. 9 in Saenger et al., 2006), and the upper 1 cm of each core was carefully extruded in the field, bagged, stored frozen prior to freeze-drying and extracted in the laboratory.

### 2.2. Microscopy

Microscopy was performed with Zeiss Axioimager A1 microscope and Zeiss AxioCam MRc Imaging system and software (Carl Zeiss GmbH, Germany).

Identification of microbial morphotypes was done in accordance with traditional phycological determination manuals (Geitler, 1932; Komárek and Anagnostidis, 1999; Castenholz, 2001; Komárek and Anagnostidis, 2005).

### 2.3. Analysis of water $\delta D$ values

Water samples were analyzed for their hydrogen isotopic composition at Dartmouth College using an H-Device (ThermoFisher, Bremen, Germany) connected to a Delta<sup>plus</sup>XL Isotope Ratio Mass Spectrometer (IRMS, ThermoFisher, Bremen, Germany). Values were corrected to the VSMOW scale, using two laboratory standards with values of -69.4‰ and -234.4‰ (previously calibrated to VSMOW and SLAP) and the VSMOW standard (0‰). Precision of water  $\delta D$  measurement was 0.5‰. A detailed description of the water isotopes measurement procedure can be found in Zhang and Sachs (2007).

### 2.4. Sample preparation and biomarker identification and quantification

Between 0.5 and 5 g of dried sediment or mat material was extracted with an Accelerated Solvent Extractor (ASE 200, Dionex Corp., Sunnyvale, CA, USA) with dichloromethane at 100 °C and 103 bar (1500 psi) for 5 min in each of 3 cycles. Total lipid extracts were blown dry under a stream of N<sub>2</sub>. A subset of 17 samples was extracted separately using the same conditions in order to conduct compound-specific isotope analyses. Silica gel chromatography was used to separate total lipid extracts into hydrocarbons (hexane) and more polar materials (dichloromethane and methanol). The hydrocarbon fraction was analyzed on a GC-MSD (Agilent GC 6890N connected to an Agilent MSD5975 detector, Agilent, Santa Clara, CA, USA) to identify lipids and assess their purity,

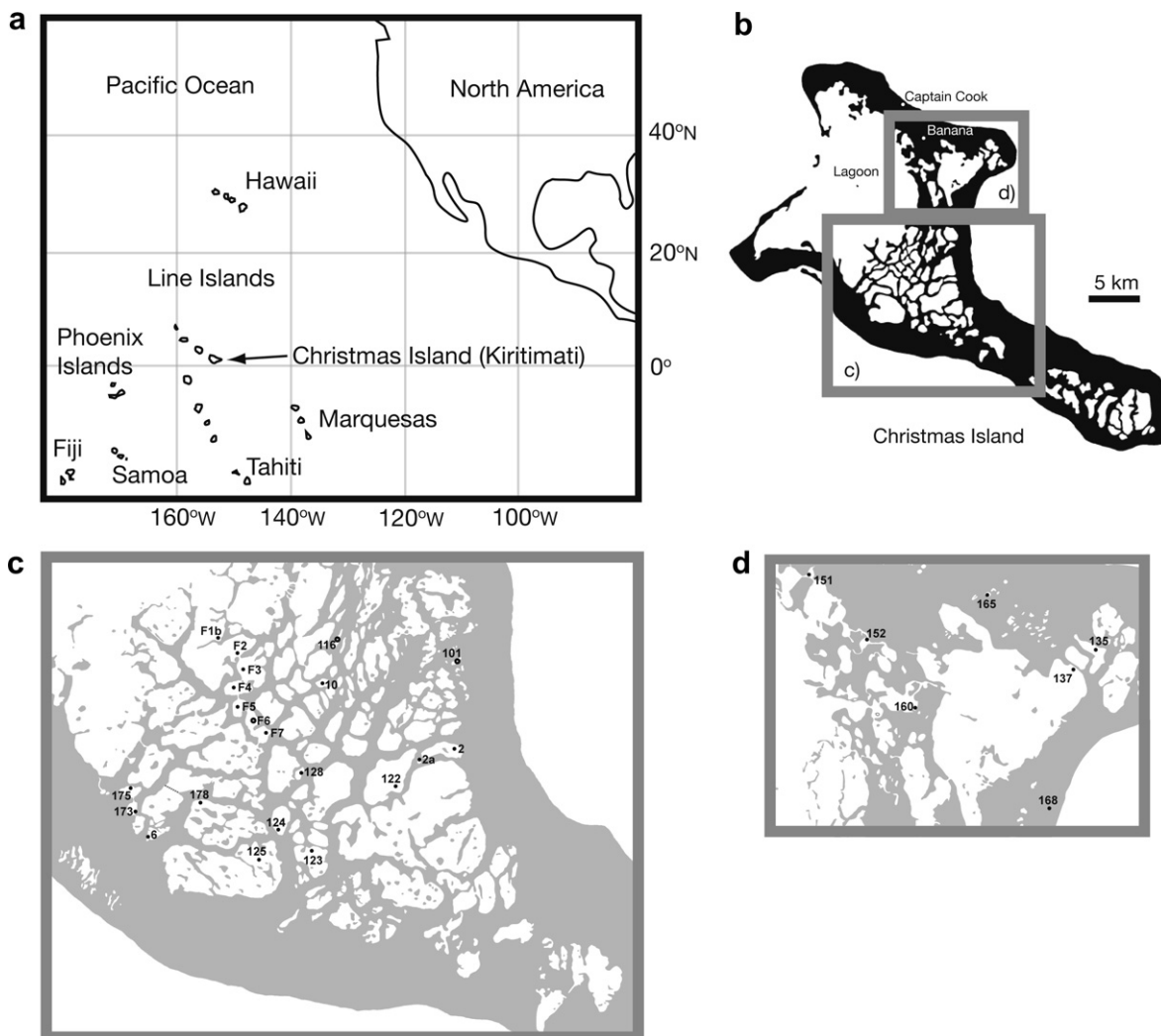


Fig. 1. Sampling location and sites. (a) Location of Christmas Island (or Kiritimati) in the Central Tropical Pacific. (b) Overview of Christmas Island. (c and d) Location of the sampled hypersaline ponds, with site numbers, map modified after Saenger et al. (2006).

then quantified on a GC-FID (Agilent GC 6890N with an FID detector) using an external standard mixture of *n*-alkanes (*n*-C<sub>14</sub> to *n*-C<sub>36</sub>).

### 2.5. Analysis of $\delta D$ values of total lipid extracts

About 100  $\mu\text{g}$  of each total lipid extract (TLE) was transferred into silver capsules (Costech, Valencia, CA, USA) using  $\text{CCl}_4$ —to avoid contamination by solvent-derived hydrogen. Folded capsules were loaded into a Costech Zero Blank Auto-sampler connected to a Thermo/Finnigan thermochemical elemental analyzer (TC/EA) (ThermoFisher, Bremen, Germany), where they were pyrolyzed at 1400  $^{\circ}\text{C}$  to  $\text{H}_2$  gas.  $\text{H}_2$  gas was introduced into a Thermo Electron Corp. Delta V Plus isotope-ratio mass spectrometer (irMS) via a ConFlo III combustion interface (ThermoFisher, Bremen, Germany). After each sample was analyzed in triplicate,  $\delta D$  values were normalized to the VSMOW scale using two laboratory standards (UWB-1, benzoic acid,  $\delta D = -64.9\text{‰}$  and a *n*-C<sub>28</sub> alkane,

$\delta D = -232.5\text{‰}$ , that had previously been calibrated to organic reference materials obtained from A. Schimmelmann, University of Indiana) and measured after every six samples. A scale stretch and drift correction (Werner and Brand, 2001) was applied for each sequence (typically 16 samples, including a blank). The average standard deviation ( $\sigma$ ) of all measured samples was 3.8‰.

### 2.6. Analysis of $\delta D$ values on specific lipids

One microliter of the hydrocarbon fraction dissolved in hexane was injected into a TraceGC II gas chromatograph (ThermoFisher, Rodano, Italy) equipped with a DB5ms column (60 m; ID: 0.32 mm; film thickness: 0.25  $\mu\text{m}$ , Agilent). The split/splitless injector was operated in splitless mode at 280  $^{\circ}\text{C}$ . The oven was programmed from 80 to 170  $^{\circ}\text{C}$  at 20  $^{\circ}\text{C}/\text{min}$  and then to 325  $^{\circ}\text{C}$  at 3  $^{\circ}\text{C}/\text{min}$ , where it was held for 20 min. The effluent from the GC entered a high-temperature conversion oven at 1400  $^{\circ}\text{C}$  to pyrolyze the sample quantitatively to  $\text{H}_2$  gas (Burgoyne and Hayes,

Table 1

Physico-chemical properties of the investigated lakes and sampled material, data taken from Saenger et al. (2006)

Lake	Sampled material	Salinity	Temperature (°C)	Conductivity (μS)	Resistance (Ω)	TDS	DO (% sat)	DO (mg/l)	Lake depth (m)	pH	Ox Red pot (mV)	NTU turbidity
168	Sediment	13.6	34.6	22820	37.05	14.83	83.6	5.44	0.30	8.09	33.3	24.2
151	Sediment	38.5	25.9	57761	17.04	37.53	98.7	6.45	0.30	8.14	−24.6	11.3
160	Sediment	38.8	29.4	58353	15.79	37.92	66.8	4.14	0.41	8.29	46.2	12
152	Sediment	39.4	26.5	59072	16.49	38.41	93.7	6.01	0.27	8.15	46.8	18
F1b	Sediment	41.2	31.8	61580	14.36	40.01	26.0	1.57	0.15	8.15	39.9	1.2
F2	Mat	41.6	25.7	61765	16.00	40.16	88.2	5.66	0.17	7.52	100.2	3.9
F3	Mat	62.9	29.8	88785	10.32	57.66	126.4	6.75	0.23	7.44	75.5	33.6
165	Sediment	63.4	34.5	92032	9.20	59.82	125.2	6.16	0.23	8.88	−12.6	40.1
F4	Mat (layer 1 & 2)	80.3	29.8	108809	8.41	70.77	60.7	2.88	0.25	7.60	74.0	4.4
F5	Mat	86.9	30.3	116102	7.81	75.54	113.9	5.31	0.20	7.84	74.8	5
101	Mat (layer 1 & 2)	87.6	32.6	117369	nd	76.19	140.7	6.41	nd	7.64	108.0	nd
123	Sediment	98.0	29.6	128117	7.17	83.28	94.7	4.18	0.28	7.75	97.4	6.7
125	Sediment	99.6	29.8	129812	7.06	84.38	87.4	3.81	0.39	7.88	36.0	6.4
175	Mat	102.6	31.3	133091	6.71	86.53	67.2	2.83	0.27	7.99	34.9	4.1
2	Mat	103.8	30.5	134453	6.71	87.34	96.8	4.10	0.29	7.83	13.0	5.9
6	Mat	104.6	31.7	135295	6.55	88.05	90.0	3.71	0.20	7.67	35.3	23.5
173	Mat	108.7	30.0	139350	6.57	90.59	69.9	2.90	0.41	7.84	42.1	4.0
F7	Sediment	114.9	31.2	146125	6.10	94.82	73.7	2.99	0.24	7.03	57.7	4.2
116	Sediment & mat	115.2	32.0	145933	6.04	94.86	124.2	4.85	0.22	7.53	66.4	4.4
2A	Mat	116.0	33.8	146559	5.83	95.17	125.6	4.78	0.19	7.90	42.8	7.5
F6	Mat	116.5	29.6	147124	6.25	95.55	36.3	1.45	0.40	7.95	50.5	5.1
10	Sediment	118.6	30.7	14932	6.04	97.02	95.2	3.68	0.65	8.03	36.1	−8.8
178	Mat	125.4	30.5	155860	5.80	101.30	72.2	2.77	0.47	7.90	38.3	8.8
137	Sediment	133.3	29.7	163302	5.62	106.10	99.4	3.61	0.49	8.02	53.0	−9.4
128	Sediment (above & below salt crust)	135.6	31.7	166460	5.14	107.00	7.0	2.30	1.71	6.80	−298.9	243.0
135	Sediment	138.8	28.2	168262	5.60	109.40	88.5	3.17	0.34	7.86	62.7	−8.5
124	Mat	146.0	30.8	175109	5.14	113.80	91.3	3.04	0.36	7.65	90.5	6.0
122	Mat	149.2	29.9	177920	5.14	115.60	82.0	2.73	0.30	7.51	119.0	11.0

1998; Hilkert et al., 1999). The H<sub>2</sub> gas was transferred via a Thermo/Finnigan GC/TC high-temperature conversion interface (ThermoFisher, Bremen, Germany) to a Thermo Electron Corp. Delta V Plus isotope-ratio mass spectrometer (IRMS) (ThermoFisher, Bremen, Germany).

The H<sub>3</sub><sup>+</sup> factor, monitoring the contribution of H<sub>3</sub><sup>+</sup> ions formed by molecule-ion interactions (H<sub>2</sub><sup>+</sup> and H<sub>2</sub>) in the ion source (Sessions et al., 2001), was determined daily and stayed nearly constant at 4.55 ( $\sigma = 0.08$ ) over 2 weeks of measurements. Each sample was measured three times.  $\delta D$  values were corrected to the VSMOW scale, by using an *n*-alkane standard mixture (*n*-C<sub>14</sub> to *n*-C<sub>36</sub>) with known isotopic composition measured after every two samples (6 GC runs). Additionally, *n*-C<sub>14</sub> and *n*-C<sub>36</sub> alkanes with a known D/H ratio obtained from A. Schimmelmann, University of Indiana, were co-injected with each sample to monitor the performance of the correction—using the external standard mixture (mean standard deviation for these two compounds was 5.6‰). The average standard deviation ( $\sigma$ ) for all measured standard mixtures was 3.5‰ ( $n = 1254$ ; 66 runs with 19 peaks each). The average standard deviation for the sample peaks was 4.1‰ ( $n = 46$ ).

### 3. RESULTS AND DISCUSSION

#### 3.1. $\delta D$ values of lake water

The hydrogen isotopic composition of water in the saline ponds of Christmas Island varied by 11.8‰, from +4.0‰ to +15.8‰ (Fig. 3 and Table 3), over the salinity range 38.5 to 149.2 (practical salinity units). Lake water with a salinity of 13.6 in lake 168, received groundwater from a freshwater lens, which had a  $\delta D$  value of −7.6‰. The lowest  $\delta D$  values for water with salinities greater than seawater (>38), +5.4‰ and +4.0‰, were found in the least and most saline lakes respectively (Fig. 3).  $\delta D$  values reached a maximum at a salinity of approximately 60 and declined above that value.

In low humidity environments, an increase in salinity resulting from an excess of evaporation over precipitation is usually accompanied by an increase in water  $\delta D$  values, according to the Rayleigh distillation model (Craig and Gordon, 1965). However, under high humidity conditions, which commonly exist on oceanic islands, (deuterium-depleted) atmospheric moisture exchanges with the evaporating liquid in the air–water boundary layer. Depending on

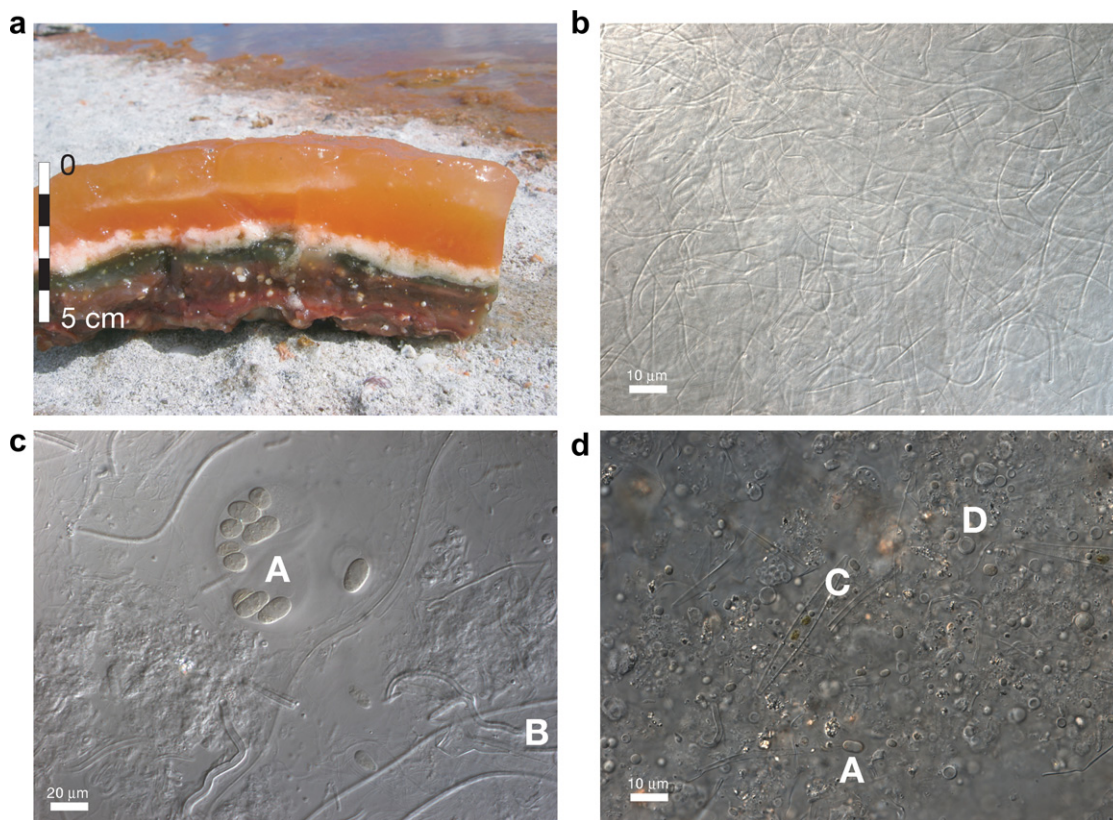


Fig. 2. (a) Photograph of a typical microbial mat encountered in the Christmas Island hypersaline ponds (here shown for lake F6). For lipid analysis the upper layer (e.g., the first 1–2 cm) was sampled. (b) Microscopic image (63 $\times$ ) of the upper layer (0–1 cm) of the microbial mat from lake F6, showing filamentous cyanobacteria (including their sheaths) of the *Phormidium/Leptolyngbia* type. (c) Microscopic image (100 $\times$ ) of the upper layer (0–1 cm) of the microbial mat from lake F3: A: coccoid cyanobacteria of the *Aphanothece* type; B: sheaths from *Phormidium/Leptolyngbia* type cyanobacteria. (d) Microscopic image (63 $\times$ ) of the upper layer (0–1 cm) of the microbial mat from lake 2A, A: coccoid cyanobacteria of the *Aphanothece* type; C: diatom (*Nitzschia*), D: coccoid cyanobacteria of the *Aphanocapsa* type. All microscopy images were taken in phase contrast mode.

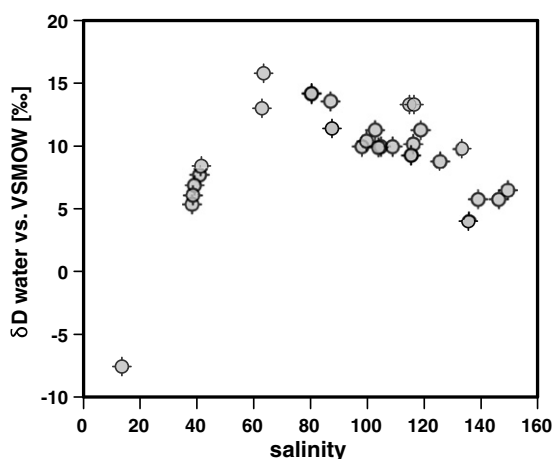


Fig. 3.  $\delta D$  values of water in the Christmas Island saline ponds plotted against salinity.

the relative humidity, there is an upper limit to deuterium enrichment in the water. At very high salinities, the effect of solutes contributed to D-depletion in water, as the ther-

modynamic activity of water decreased, effectively reducing the humidity contrast and the rate of evaporation (Gonfiantini, 1986). In addition, the hydration sheath for polyvalent ions became enriched in deuterium relative to the free water such that, in the last stages of evaporation, as salts precipitate, this D-enriched water was removed from free water and preserved in the hydration water of salts (Gonfiantini, 1986). The observed decrease in  $\delta D$  values, at higher salinities in the Christmas Island ponds was consistent with the combined action of these processes. From the standpoint of paleoclimate and paleoenvironmental reconstructions, the polynomial shape of the salinity vs.  $\delta D_{\text{water}}$  curve limits the estimation of salinity from water  $\delta D$  values (to the extent that the latter can be determined) in humid environments when salinities are  $\sim 60$  or greater.

### 3.2. Lipid identification, concentration, and biological origin

Samples from 17 lakes on Christmas Island were analyzed for their lipid composition to determine the dominant organic matter sources (Table 2). In most samples, the concentration of all lipids in the hydrocarbon fraction was higher in microbial mats than in surface sediments. Lipid

Table 2  
Concentration of the specific lipids in the analysed samples (in  $\mu\text{g/g}$  dry sediment)

Lake	Salinity	<i>n</i> -C <sub>17</sub>	<i>n</i> -C <sub>17:1</sub>	<i>n</i> -C <sub>18</sub>	<i>n</i> -C <sub>18:1</sub>	Phytene	Diploptene
151	38.5	0.06	0.12				
F3	62.9	n.d.		n.d.			
165	63.4	n.d.			n.d.	n.d.	
101	87.6	12.94	5.79				
123	98.0	3.45		0.72			
125	99.6	0.86	0.37				
K6	104.6	3.79		0.94			
173	108.7	3.06		0.22		0.45	
116	115.2	5.38					
2A	116.0	1.16			0.25	0.17	
K10	118.6	2.28	0.33		0.29		0.43
178	125.4	4.99					
128	133.8	0.31			0.25		
137	133.3	0.35					
135	138.8	1.14			1.36	1.15	
124	146.0	1.52			0.56	0.25	0.47
122	149.2	0.18					

composition in the two types of material was similar, suggesting similar sources of organic matter. The most abundant lipid in the hydrocarbon fraction in all samples was the *n*-C<sub>17</sub> alkane, except for the mat sample from lake F3, where *n*-C<sub>18</sub> was most abundant. The concentration of *n*-C<sub>17</sub> varied between 0.06 and 12.9  $\mu\text{g/g}$  dry sediment (Table 2). The second most abundant lipids were often the *n*-C<sub>17:1</sub> and *n*-C<sub>18:1</sub> alkenes; other lipids such as the *n*-C<sub>18</sub> alkane were much less abundant. Five samples had significant amounts of phytene (0.17 to 1.15  $\mu\text{g/g}$  sediment) and diploptene was present in moderate amounts in two samples (0.43 and 0.47  $\mu\text{g/g}$  sediment).

Overall, the identified hydrocarbons in the Christmas Island mats and sediments were typical for cyanobacterial organic matter, similar to other reports (Shiea et al., 1991; Sakata et al., 1997; Simoneit et al., 1998; Dembitsky and Srebnik, 2002; Jahnke et al., 2004; Pancost et al., 2005). *n*-C<sub>17</sub> alkanes and alkenes are usually the major hydrocarbons in cyanobacterial mats (Arp et al., 1999). Grimalt et al. (1992) identified these hydrocarbons plus *n*-C<sub>18</sub> alkanes and alkenes, phytene, and diploptene, in concentrations similar to those observed in our study. These mats formed by the filamentous cyanobacterium *Phormidium*, which was identified in several of the Christmas Island mats by light microscopy (Fig. 2). The aliphatic lipids we found (*n*-C<sub>17</sub>, *n*-C<sub>17:1</sub>, *n*-C<sub>18</sub>, *n*-C<sub>18:1</sub>), occurred in the membranes of cyanobacterial cell walls and were likely synthesized via the acetogenic pathway through elongation of an acetyl-CoA precursor. In higher plants this is achieved through decarboxylation of the resulting fatty acid (Kolattukudy, 1967; Kolattukudy, 1981), a mechanism possibly operating in cyanobacteria.

Phytene is an intermediate product in the transformation of the phytol side-chain of chlorophyll *a* to phytane (Ikan et al., 1975; Grossi et al., 1998). Since no higher plant biomarkers, such as long-chain *n*-alkanes (*n*-C<sub>25</sub> to *n*-C<sub>33</sub>), were observed in the sediments, and the vegetation cover on the Island was limited to sparse grasses and shrubs, we concluded that the phytene was of cyanobacterial origin. Phytol is produced via the 2-*C*-methyl-*D*-erythritol 4-phos-

phate/1-deoxy-*D*-xylulose 5-phosphate or DOXP/MEP pathway (Rohmer et al., 1993; Schwender et al., 1996) with isopentenyl pyrophosphate (IPP) as a precursor.

Diploptene, generally assumed to be derived from prokaryotes (Rohmer et al., 1984), is an abundant hopanoid in cyanobacteria (Derosa et al., 1971; Sakata et al., 1997). In coastal settings a terrestrial (soil) origin of diploptene has been suggested (Prahl et al., 1992). Due to the absence of extensive vegetation cover and/or soil on Christmas Island, and the lack of higher plant biomarkers in our sediment samples, diploptene was assumed to be of cyanobacterial origin. These lipids share a common biosynthetic origin with sterols, the MVA (mevalonate) or Bloch-Lynen pathway (Chaykin et al., 1958; Lynen et al., 1958).

### 3.3. Individual lipid $\delta\text{D}$ values

Due to the similarity of  $\delta\text{D}$  values in lipids produced by a single biosynthetic pathway (e.g., acetogenic, DOXP/MEP, and MVA), we discuss our results by grouping lipids according to their biosynthetic origin. Also, because there were no apparent differences in  $\delta\text{D}$  values obtained from sediments or microbial mat materials we have combined the discussion.

#### 3.3.1. Acetogenic lipids (hydrocarbons)

$\delta\text{D}$  values of acetogenic hydrocarbons in ponds (*n*-C<sub>17</sub>, *n*-C<sub>17:1</sub>, *n*-C<sub>18</sub>, *n*-C<sub>18:1</sub>) varied by more than 100‰, from  $-173\text{‰}$  to  $-57\text{‰}$  (Table 3).  $\delta\text{D}$  values of *n*-C<sub>17</sub>, *n*-C<sub>17:1</sub>, and *n*-C<sub>18:1</sub> were very similar within a single sample. The *n*-C<sub>18</sub> alkane, which was only found in sufficient concentrations for isotope measurements in four samples, was always depleted in deuterium relative to other hydrocarbons (by 27‰ to 66‰).  $\delta\text{D}$  values for each compound were positively correlated with salinity.  $\delta\text{D}$  values for the *n*-C<sub>17</sub> alkane, the major hydrocarbon in all samples, increased by 80‰ over a salinity range of 110. The most negative  $\delta\text{D}$  value for *n*-C<sub>17</sub> ( $-141\text{‰}$ ) was measured in the least saline sample (Lake 151) with a salinity of 38.5, while the highest  $\delta\text{D}$  value for *n*-C<sub>17</sub>,  $-57\text{‰}$ , was measured in Lake 124 (salinity of 146).

Table 3  
 $\delta D$  values for the analyzed lipids from the Christmas Island saline lakes

Lake	Salinity	$\delta D$ water (‰)	$n-C_{17}$	Stdev	$n-C_{17:1}$	$n-C_{18}$	Stdev	$n-C_{18:1}$	Stdev	Phytene	Stdev	Diploptene	Stdev	TLE	Stdev
151	38.5	5.4	-141	1.5 <sup>a</sup>										-192	3.3
F3	62.9	13.0	-126	3.3		-173	4.1							-158	4.1
165	63.4	15.8	-132	1.7				-131	8.0	-276.2	3.9			-160	2.2
101	87.6	11.4	-129	1.0	-123.5	1.0								-154	3.5
123	98.0	10.0	-107	0.4		-156	5.1							-145	0.4
125	99.6	10.4	-97	2.9 <sup>a</sup>										-144	0.9
K6	104.6	10.0	-107	0.7		-166	4.9							-151	0.4
173	108.7	10.0	-100	0.7		-124	9.7			-216.2	6.3			-147	1.4
116 (mat)	115.2	9.3	-123	3.0										-84	16.6
2A	116.0	10.2	-87	3.6				-95	4.1	-215.9	5.4			-138	2.1
K10	118.6	11.3	-90	2.5	-98.4	3.4		-79	4.9			-172.7	6.0	-134	3.6
178	125.4	8.8	-90	5.5										-85	2.3
128	135.6	4.0	-56	0.6				-90	16.7					-134	3.4
137	133.3	9.8	-63	13.9										-109	4.4
135	138.8	5.8	-87	1.3	-67.0	n/a		-96	2.8	-187.0	6.1			-120	0.7
124	146.0	5.8	-57	2.9				-76	5.2	-204.3	—	-154.5	—	-122	1.7
122	149.2	6.5	-66	9.4										-92	4.0

Standard deviation is given for three replicate measurements.

<sup>a</sup> The  $n-C_{17}$  alkane and  $n-C_{17:1}$  alkene were not baseline separated in these samples, therefore peaks were integrated as one.

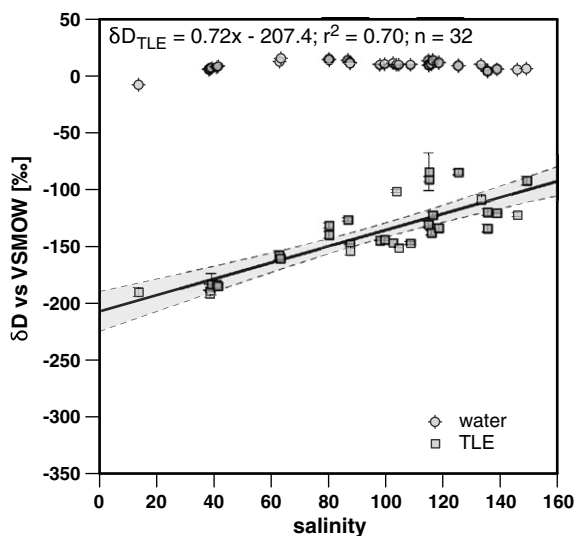


Fig. 4. Linear relationship between  $\delta D$  values of total lipid extracts (TLE) and salinity. Lake water  $\delta D$  values are shown for comparison.

There was a strong linear relationship between the  $n-C_{17}$   $\delta D$  values and salinity ( $r^2 = 0.78$ ,  $n = 17$ ) with a slope of 0.77 (Fig. 5), with a similar relationship for  $n-C_{18:1}$  ( $r^2 = 0.76$ ;  $n = 6$ ). Overall,  $\delta D$  values of acetogenic hydrocarbons showed a strong positive linear relationship with salinity, even though water  $\delta D$  values changed parabolically with salinity (Fig. 5).

The  $n-C_{18}$  alkane, which was depleted in deuterium relative to  $n-C_{17}$  on average by 50‰ (ranging from 27‰ to 66‰), indicated a different source for this lipid than the other hydrocarbons. Whether  $n-C_{18}$  was produced by a different species or was the product of a degradation process involving hydrogen exchange, cannot be determined from

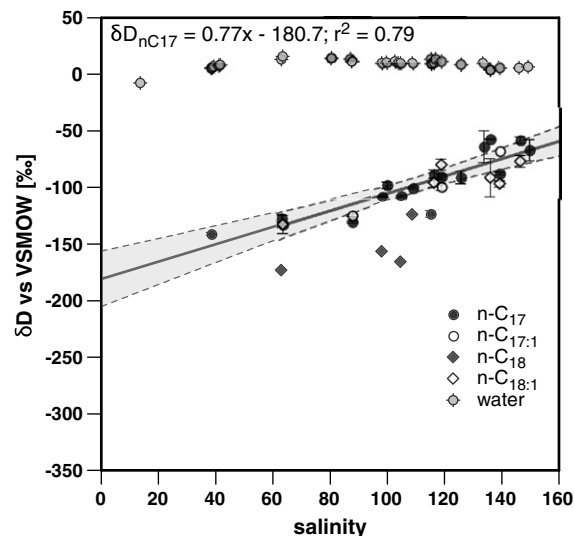


Fig. 5. Relationship between  $\delta D$  values of hydrocarbons and salinity. Water  $\delta D$  values are shown for comparison.  $1\sigma$  error bars shown for triplicate analysis of lipid  $\delta D$  values, if not visible they are smaller than the symbol. Regression line is for  $n-C_{17}$ .

our data. However,  $n-C_{18}$  was only identified in salinities up to 100, supporting the notion that it might have been derived from a different species preferring moderate salinities. There was no other statistically significant relationship between the lipid  $\delta D$  values and other physico-chemical parameters, that were independent of variations in salinity (such as lake temperature or pH).

### 3.3.2. Lipids produced via DOXP-MEP (phytene) and MVA (diploptene) pathways

Due to lower abundances of phytene and diploptene, relative to acetogenic lipids only five samples of the former and two of the latter could be analyzed isotopically. The  $\delta D$

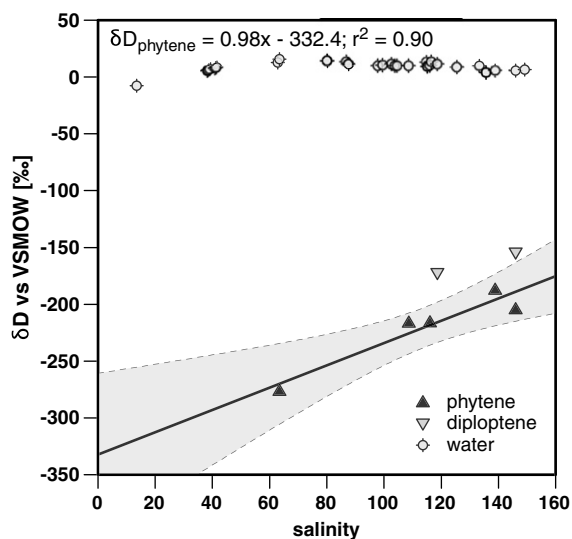


Fig. 6. Relationship between the  $\delta D$  values of phytene and diploptene vs. salinity. Water  $\delta D$  values shown for comparison. Regression line is shown for phytene.

values of phytene were between  $-276\text{‰}$  and  $-187\text{‰}$ . There was a significant positive linear relationship between salinity and phytene  $\delta D$  values ( $r^2 = 0.9$ ,  $n = 5$ ), with a slightly steeper slope than for the acetogenic lipids (0.98) (Fig. 6).  $\delta D$  values of phytene averaged  $140\text{‰}$  less than the  $n\text{-C}_{17}$  alkane, (with a range between  $166\text{‰}$  and  $110\text{‰}$ ). This is consistent with previously reported differences between phytol, phytadienes and hydrocarbons in algae (Sessions et al., 1999; Zhang and Sachs, 2007).

$\delta D$  values for diploptene were  $-172\text{‰}$  and  $-155\text{‰}$ , for the lower and higher salinity samples. Diploptene  $\delta D$  values followed the trend of all other lipids analyzed with increasing values at higher salinities, but with a slope slightly less than  $n\text{-C}_{17}$  at 0.66. With only two diploptene  $\delta D$  analyses little significance can be attributed to a different slope.

Diploptene was depleted in deuterium relative to  $n\text{-C}_{17}$  by  $97\text{‰}$  on average ( $91\text{‰}$  and  $103\text{‰}$ ), within the range reported for the differences between sterols (which are produced via the same MVA biosynthetic pathway as diploptene) and hydrocarbons (Sessions et al., 1999; Sauer et al., 2001). There was no systematic variation in these differences with salinity. The difference between the  $n\text{-C}_{17}$  alkane and phytene showed a negative correlation with temperature ( $r^2 = 0.63$ ;  $n = 5$ ), but with only five data points a causal relationship remains speculative.

### 3.3.3. Total lipid $\delta D$ values

Total lipid extract (TLE)  $\delta D$  values were between  $-192\text{‰}$  and  $-84\text{‰}$ , over a salinity range of 136 (Table 4). Sediment and mat samples from Lake 116 were extracted separately and showed no substantial isotopic difference ( $-91\text{‰}$  and  $-84\text{‰}$ , respectively). Furthermore, the upper two layers of microbial mats from Lakes 101 and F4, identified by color and microbial species composition (Stal, 1995), were analyzed separately and found to have no substantial isotopic differences (Lake 101, layer 1:  $-154\text{‰}$ ,

Table 4

$\delta D$  values for total lipids (TLE) from the Christmas Island saline lakes (only TLEs were analysed from these lakes)

Lake	Salinity	$\delta D$ water (‰)	$\delta D$ TLE (‰)	Stdev
168	13.6	-7.6	-190	3.9
160	38.8	6.1	-189	6.0
152	39.4	6.9	-183	9.7
F1b	41.2	7.7	-183	0.3
F2	41.6	8.4	-185	1.6
F4	80.3	14.2	-131	2.2
F5	86.9	13.6	-126	1.5
175	102.6	11.3	-147	nd
K2	103.8	9.9	-101	1.4
F7	114.9	13.3	-130	2.5
116 (sediment)	115.2	9.3	-91	2.3
F6	116.5	13.3	-122	2.5
101 (layer 2)	87.6	11.4	-148	0.7
F4 Mat (layer 1)	80.3	14.2	-140	3.2
128 (underneath salt crust)	135.6	4.0	-120	2.8

Standard deviation is given for three replicate measurements.

layer 2:  $-148\text{‰}$ ; Lake F4, layer 1:  $-140\text{‰}$ , layer 2:  $-131\text{‰}$ ). Conversely, a sample taken under a halite crust on the bottom of Lake 128, was enriched by  $14\text{‰}$  compared to a sample from above the salt crust, likely resulting from more saline conditions.

TLE  $\delta D$  values were positively correlated with salinity ( $r^2 = 0.70$ ;  $n = 32$ ) with a slope of 0.72, similar to that for the  $n\text{-C}_{17}$  alkane (0.77) (Fig. 4). TLE  $\delta D$  values were more negative by  $39\text{‰}$ , on average, relative to the  $n\text{-C}_{17}$  alkane within the same sample, but more enriched in deuterium compared to phytene (by an average of  $107\text{‰}$ ) and diploptene (by  $43\text{‰}$ ). TLEs represent a mixture of compounds from the three major lipid biosynthetic pathways, with a large contribution from the acetogenic lipids (e.g., fatty acids and hydrocarbons). The smaller  $r^2$  value for the TLE  $\delta D$  vs. salinity regression, compared to the  $n\text{-C}_{17}$  alkane, presumably reflected varying contributions from the lipid biosynthetic pathways and varying inputs from non-cyanobacterial lipids. However, the strong correlation between TLE  $\delta D$  values and salinity suggested that the majority of lipids in our samples had a similar, presumably cyanobacterial, source, or that a range of organisms responded similarly to changes in salinity.

### 3.4. Lipid–water D/H fractionation and its relationship to salinity

There was an increase of cyanobacterial lipid  $\delta D$  values by more than  $100\text{‰}$ , over a salinity range of 136. Conversely, water  $\delta D$  values varied by just  $12\text{‰}$  and were not correlated with salinity, which strongly implied a decrease in net D/H fractionation between source water and lipids (or increase in fractionation factors  $\alpha_{\text{lipid-water}}$  or  $\epsilon_{\text{lipid-water}}$ , with  $\alpha = (1000 + \delta_{\text{lipid}})/(1000 + \delta_{\text{water}})$ ;  $\epsilon = 1000 * ((\delta_{\text{lipid}} + 1000)/(\delta_{\text{water}} + 1000) - 1)$ ). When plotting  $\delta D$  values of water vs.  $\delta D$  values of lipids, relationships with negative slopes were obtained for all lipids (significant only for

$n\text{-C}_{17:1}$ ,  $r^2 = 0.81$ ,  $n = 4$ ; and phytene  $r^2 = 0.91$ ,  $n = 5$ ). However, seemingly large and negative  $\alpha_{\text{lipid-water}}$  values ( $-2.9$  to  $-8.1$ ) were obtained from the slopes of these regressions.  $\alpha_{\text{lipid-water}}$  values derived from the intercepts of these regressions were 0.980 for  $n\text{-C}_{17:1}$  and 0.854 for phytene. In a simple one-component (i.e., single hydrogen source) system, the intercept of a  $\delta D_{\text{water}}$  vs.  $\delta D_{\text{lipid}}$  relationship represented  $\epsilon_{\text{lipid-water}}$  and the slope  $\alpha_{\text{lipid-water}}$  (i.e.,  $\delta D_{\text{lipid}} = \alpha \delta D_{\text{water}} + \epsilon$ ), whereby both fractionation factors should have yielded the same value ( $\epsilon = \alpha - 1$ ) (Sessions and Hayes, 2005). On the contrary, calibration studies on batch cultures and natural systems have demonstrated that such a simple model was inadequate for hydrogen isotopes in algae (Zhang and Sachs, 2007).

The stark disagreement between slope- and intercept-derived fractionation factors in Christmas Island microbial mat lipids implied that more than one fractionation process or hydrogen source contributed to the observed net D/H fractionation (Sessions and Hayes, 2005) and that the isotopic composition of the source water was not the parameter determining the  $\delta D$  value of the lipids investigated here, as its isotopic composition did not change substantially. Nevertheless, net isotopic fractionation between source water and lipids decreased (fractionation factor  $\alpha$  increased) in all three compound classes with increasing salinity and showed strong linear correlations (Fig. 7). Differences in  $\alpha_{\text{lipid-water}}$  for lipids derived from the three biosynthetic pathways remained almost constant over the entire salinity range as indicated by the similar slopes of the regressions (0.00080 to 0.00107).

Isotopic differences between the three compound classes were within the ranges reported in the literature; acetogenic

lipids are least depleted in deuterium (Sessions et al., 1999; Sauer et al., 2001). Acetogenic biosynthesis starts with the production of pyruvate, (a product of the Calvin Cycle) from which acetyl-CoA is derived, the building block for aliphatic lipids (Kolattukudy, 1967; Kolattukudy, 1981; Chikaraishi et al., 2004). Lipids produced via the MVA pathway, such as diploptene, are derived from pyruvate, which is converted to 3-hydroxy-3-methylglutaryl-CoA (HMG-CoA), reduced to mevalonic acid (MVA) by HGM-CoA reductase, transformed into farnesyl diphosphate (FPP), and finally to squalene (Lange et al., 2000; Chikaraishi et al., 2004). Squalene is the precursor to all sterols and hopanoids, including diploptene.

The most deuterium-depleted lipids, such as phytol, are produced via the DOXP/MEP pathway (Rohmer et al., 1993; Schwender et al., 1996; Lichtenthaler, 2004). DOXP is produced by pyruvate and glyceraldehydes-3-phosphate (GA-3P) from the Calvin Cycle. DOXP is converted into MEP, and then transformed into isopentyl diphosphate (IPP). Phytol is ultimately formed from geranylgeranyldiphosphate (GGPP) through the elimination of three carbon-carbon double bonds (see discussion in Zhang and Sachs (2007), and references therein). It is currently unknown at which biosynthetic step and by which mechanism hydrogen isotope fractionations arise that deplete isoprenoids in deuterium (compared to acetogenic lipids). Isotopically different pools of NADPH have been suggested to exist, as well as additional, yet unknown fractionation steps in the DOXP/MEP pathway, see discussion in Sessions et al. (1999).

Intercept values for the  $\alpha_{\text{lipid-water}}$  vs. salinity relationship (corresponding to a fractionation at zero salinity) are

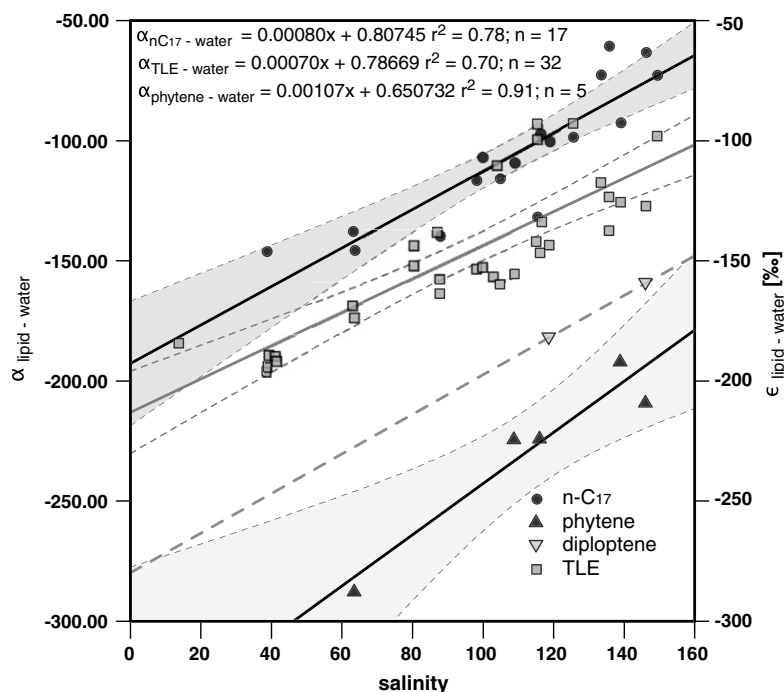


Fig. 7. Relationship between the isotopic fractionation (given as  $\alpha$  and  $\epsilon$  values) of three lipid biomarkers ( $n\text{-C}_{17}$ , phytene, diploptene) and the TLEs from which those lipids were purified, plotted as a function of salinity.

lower, or at the lower end of reported values, for all compound classes analyzed. A possible explanation for this observation could be that different species exhibit different D/H fractionation during lipid synthesis, as demonstrated for different species of cultured green algae (Zhang and Sachs, 2007), and/or a shifting cyanobacterial population in the ponds and microbial mats as salinity increased. An alternative explanation is that the relationship between salinity and  $\alpha_{\text{lipid-water}}$  might cease to be linear at lower salinities. In fact, when applying a polynomial (2nd order) regression to the relationship between  $\alpha_{n\text{-C}_{17}\text{-water}}$  and salinity, a higher  $r^2$  of 0.84 is obtained with an intercept of 0.860, within the range of previously reported values (Sessions et al., 1999; Sachse et al., 2004). Also, the  $\alpha_{\text{lipid-water}}$  values for total lipid extracts for the six low-salinity ponds (salinities from 13.6 to 41.6) were very similar (0.806 to 0.816). The small number of samples analyzed from other compound classes did not permit such an evaluation, nor did our calibration have sufficient data points at low salinities to confirm a possible polynomial relationship.

The importance of species-specific differences was further evident when comparing our calibration curve to data from two haptophyte marine algae, *E. huxleyi* and *G. Oceanica* (Schouten et al., 2006). Schouten et al. (2006) analyzed the isotopic fractionation between source water and alkenones, biomarkers specific to these algae, over a salinity range from 24.8 to 35.1. Although this was a much narrower salinity range an increase in  $\alpha_{\text{lipid-water}}$  of 0.003 for a salinity range of one was observed, which is steeper by a factor of about four than the slope of 0.0008 for the Christmas Island  $n\text{-C}_{17}$  and TLE vs. salinity relationships (0.001/per salinity range of one for phytene). However, both data sets are not fully comparable since Schouten et al. (2006) reported variable growth rates (from 0.4 to  $1.4 \text{ d}^{-1}$ ) that also correlated with  $\alpha_{\text{lipid-water}}$ .

In the microbial mat ecosystems of Christmas Island one can assume a comparable distribution of growth rates, given similar light, temperature, and nutrient levels. However, it has been shown that photosynthetic activity in cyanobacterial mats can decrease as salinity increases (Garcia-Pichel et al., 1999). Yet, studies on halotolerant cyanobacteria, such as members of the *Aphanothece* genus, which were identified in our Christmas Island mats by light microscopy (Fig. 2), have shown that growth rates were low and constant throughout a salinity range of 30–210 (Garcia-Pichel et al., 1998). The tendency to form gelatinous coverings also supports a slow but steady growth. The maximal range of growth rates for halotolerant cyanobacteria varied only by  $0.4 \text{ d}^{-1}$  for a salinity range of 0 to 250 ppt (Garcia-Pichel et al., 1998; Nübel et al., 2000). Assuming the (steepest) calibration curve presented by Schouten et al. (2006) for growth rate dependency of  $\alpha_{\text{lipid-water}}$ , a decrease of  $0.4 \text{ d}^{-1}$  in growth rate would result in an increase of only about 0.028  $\alpha$  units (i.e., an  $\epsilon_{\text{lipid-water}}$  increase of 28‰). Although species-specific differences were to be expected, it is unlikely that such small changes in growth rate, as observed in halotolerant cyanobacteria, can account for the changes in  $\alpha$  observed in the Christmas Island mats. The majority of the observed 0.083 increase in  $\alpha$  (or increase in  $\epsilon_{\text{lipid-water}}$  of 83‰), over a salinity range of

136 in Christmas Island ponds, must have been causally related to the salinity increase itself.

### 3.5. Mechanisms for decreasing net fractionation during increasing salinity

When salinity (the total mass of ions per unit mass of water) in a closed water body increased, a number of chemical and physical parameters were also affected (Javor, 1989). For example, vapor pressure and activity of water (defined as vapor pressure of water divided by vapor pressure of pure water) decreased. Water activity has been shown to be an important controlling factor of the ecophysiology of microorganisms in hypersaline brines (Javor, 1989). Diffusivity, solubility of gases, and the specific heat all decreased with increasing salinity, whereas viscosity increased. As these physical properties did change with salinity, cells were subjected to osmotic gradients. It has been shown that green algae did alter their membrane fatty acid composition in response to increasing osmotic pressure, whether ionic (e.g., salinity) or molecular (e.g., sorbitol) in origin (Xu et al., 1998). Additionally, pH and alkalinity can be affected, depending on the nature of the ions present. Thus, it is likely that the combined action of these processes, across steep salinity gradients affected the metabolism of the microorganisms of Christmas Island lakes.

While our experiment did not allow us to identify or link these effects to the observed changes in D/H fractionation between water and lipids, the similarity of the slopes and consistent isotopic differences between lipids from the three biosynthetic pathways suggested that biological control over the  $\alpha_{\text{lipid-water}}$ –salinity relationship, was exerted before the last common biosynthetic branching point. The last common precursor molecule to all three biosynthetic pathways was pyruvate, which was produced from 3-phosphoglyceric acid (3-PGA), and originated in the Calvin cycle. Hydrogen was added from NADPH, when 3-PGA was converted to GA-3-P. This and the variety of chemical and physical properties that change with salinity lead us to hypothesize that the cause for the  $\alpha_{\text{water-lipid}}$  dependency on salinity is not in the lipid biosynthesis itself, but rather in the transport of water into the cell.

There are at least two modes of water transport into cells. The primary mode of water transport into cells was believed to be diffusion through cell walls (Haines, 1994). However, in the 1990s it was discovered that a number of organisms, including plants and cyanobacteria, possess water channels within their cell walls, called aquaporins (Agre et al., 1993; Chrispeels and Agre, 1994; Tanghe et al., 2006), where water enters and leaves the cell through facilitated diffusion (e.g., along concentration gradients). Proton and ion channels constitute an additional means of (active) transport for hydrogen into and out of cells (so-called  $\text{Na}^+/\text{H}^+$  antiporters) (Waditee et al., 2001).

It has been shown that aquaporins play an essential role in regulating water transport into the cell, especially during periods of (environmental) stress. Saltwater outside the cell generated an osmotic pressure gradient, drawing water out of the cell. Aquaporins were downregulated or closed to prevent water loss from cells, which has been demonstrated

in plants exposed to saltwater (Boursiac et al., 2005). Thus, ambient water is not necessarily the same as intracellular water from which hydrogen is derived for biosynthetic reactions. In fact a recent study on the heterotrophic bacterium *Escherichia coli* showed that up to  $53 \pm 12\%$  of the hydrogen from can be isotopically distinct from ambient water (Kreuzer-Martin et al., 2006)—due to internal water produced from metabolic reactions. A decreasing net D/H isotopic fractionation requires a deuterium-enriched intracellular water.

To explain how intracellular water becomes more deuterium-enriched than ambient water two mechanisms are conceivable:

1. It may be there is less fractionation against HDO during water transport into the cell at higher salinities. However, even if such a process takes place, it is unlikely that the heavier molecules (HDO instead of H<sub>2</sub>O) of water, or D<sup>+</sup> instead of H<sup>+</sup> ions, are preferentially transported into the cell. Indeed, certain proton channels (e.g., voltage gated channels) have been shown to fractionate against deuterium (DeCoursey, 2003), resulting in the opposite isotope effect.
2. A more likely process is that under high salinities less water is exchanged through the membrane and the metabolic water inside the cell is continuously “recycled”. Studies on cyanobacteria have shown that under salt stress the volume of water in the cytosol of cyanobacteria decreases by as much as 25% (Allakhverdiev et al., 2000a,b). Aquaporins and Na<sup>+</sup> channels are restricted after exposure to high salinities to maintain non-toxic levels of Na<sup>+</sup> inside the cell (Pomati et al., 2004; Boursiac et al., 2005). Thus, any isotopic enrichment of the remaining intracellular water is due to continuous recycling of this water, as a variety of metabolic reactions produce water. A continuous removal of deuterium-depleted hydrogen from intracellular water during NADPH production must enrich the residual water pool with deuterium, if the rate of hydrogen extraction from that pool is large relative to the rate of hydrogen replenishment (from ambient water).

Biosynthetic fractionation during lipid biosynthesis itself might not be affected directly by salinity at all, as evidenced by the constant isotopic differences of products from three biosynthetic pathways. However, net D/H fractionation between all lipids and water decreased. Therefore, deuterium enrichment in the intracellular water would explain the observed D-enrichment of cyanobacterial lipids as salinity increased. Experimental studies comparing the isotopic composition of intra and extracellular water and its relationship to salinity are needed to confirm the operation of such a mechanism.

An additional reason for the observed increase in lipid  $\delta D$  values with increasing salinity may lie in the operation of “dark metabolism” in cyanobacteria when no light is present or under nutrient-limited conditions (Stal, 1995). Some cyanobacteria are able to accumulate large amounts of storage products, such as poly-glucose, which are used to produce energy at times when no photosynthesis is pos-

sible (e.g., anoxic or dark conditions). Glucose is converted to lactate, acetate, ethanol, CO<sub>2</sub> and H<sub>2</sub> via mixed acid fermentation (Moezelaar and Stal, 1997). Since protium should be preferentially released as H<sub>2</sub> gas, the remaining intracellular pool of hydrogen should become enriched in deuterium. We have no evidence to suggest this mechanism is operating in the Christmas Island mats, but if the dark metabolism became increasingly important as salinity increased this mechanism could enrich the intercellular hydrogen pool in deuterium.

Although, we cannot rule out possible differences in  $\alpha_{\text{lipid-water}}$  for different cyanobacterial species, we note that the strong correlation between  $\alpha_{\text{lipid-water}}$  and salinity for all lipids analyzed, as well as the constant isotopic differences between lipids produced from the three biosynthetic pathways, points to a similar behavior of  $\alpha_{\text{lipid-water}}$  for all cyanobacteria in the Christmas Island mats. Although a variety of cyanobacterial species have been observed in these microbial mats, the extremely halotolerant filamentous (*Phormidium–Leptolyngbia* genus) and coccoid (*Aphanothece* genus) cyanobacteria seem to dominate the microbial community in the Christmas Island ponds (Fig. 2). Additionally, the composition of lipids in the mats is similar to previously reported distributions for *Phormidium*-type microbial mats (Grimalt et al., 1992; Simoneit et al., 1998). Due to the high salinities the diversity of organisms capable of surviving in these environments is limited and the mats might be expected to consist of a relatively narrow range of species.

In order to establish  $\alpha_{\text{lipid-water}}$  as a proxy for salinity in paleoclimate applications, future studies should focus on other groups of organisms (such as marine algae). Schouten et al. (2006) confirmed the operation of a similar mechanism in two marine algae in batch cultures, although with a steeper slope of the  $\alpha_{\text{lipid-water}}$  vs. salinity linear regression, perhaps resulting from variable growth rates in the cultures, and/or species-specific differences in water uptake. In fact, the species-specific differences observed in  $\alpha_{\text{lipid-water}}$  for freshwater algae, as observed by Zhang and Sachs (2007), might also be related to different water uptake strategies by these algae. These results stress the importance of independent constraints on the origin of the lipids in sediments, using biomarkers with a known source.

#### 4. CONCLUSIONS

We have demonstrated for the first time that cyanobacterial lipids (hydrocarbons, diploptene and phytene as well as total lipids) from naturally occurring microbial mats became increasingly enriched in deuterium (by almost 100‰ for *n*-C<sub>17</sub> and more than 100‰ for TLEs) with rising salinity (38 to 149.2) in the absence of any substantial increase in water  $\delta D$  values. There was a strong dependency of D/H fractionation in lipids ( $\alpha_{\text{lipid-water}}$ ) on salinity. The isotopic fractionation between lipids and water decreased by about 0.8‰ to 1.1‰ for every 1 unit increase in salinity (i.e.,  $\alpha_{\text{lipid-water}}$  increased by 0.0008 to 0.001 per unit increase in salinity). These findings show that care must be exercised when using lipid  $\delta D$  values to reconstruct source water  $\delta D$  values in systems where changes in salinity might have

occurred. On the other hand, changes in lipid  $\delta D$  values could become a useful indicator of paleosalinity if additional constraints on the source water isotopic composition (e.g., using  $\delta^{18}O$  values from foraminifera or ostracods) can be made.

Since the isotopic differences between compounds produced via the three major biosynthetic pathways for lipids remain unaffected by changes in salinity, we argue the biological control over this mechanism is exerted before the last common biosynthetic branching point for these three pathways, the Calvin Cycle. As a likely mechanism for the observed decrease in net D/H fractionation at higher salinities we propose a reduced exchange with the extracellular source water owing to down-regulation of water channels (aquaporins) and consequent increased incorporation of recycled metabolic water in biosynthetic products. Metabolic or intracellular water ought to become enriched in deuterium as isotopically-depleted hydrogen is continuously removed for NADPH production (Schmidt et al., 2003), leaving D-enriched water for biosynthesis.

These results and subsequent studies could lead to the establishment of a paleo-salinity proxy based on lipid  $\delta D$  values. However, the mechanism responsible for changes in the net isotopic fractionation that accompanies salinity changes must be confirmed. Additional factors, such as the nature of the solute (NaCl vs. NaSO<sub>4</sub> for instance, which influences a number of physico-chemical parameters in the brine), species-specific differences, and the nature of  $\alpha_{\text{lipid-water}}$  at very low and very high salinities must be investigated to fully understand variations in lipid  $\delta D$  values from saline and hypersaline systems, as it is likely that D/H fractionation between source water and lipids under extremely hypersaline conditions will approach a minimum value, which might well be species-specific.

#### ACKNOWLEDGMENTS

This material is based upon work supported by the National Science Foundation under Grant No. 0639640 and by the Gary Comer Science and Education Foundation to J.P.S. The Alexander von Humboldt foundation is acknowledged for providing a Feodor-Lynen Research fellowship to Dirk Sachse. We thank Rienk H. Smittenberg, Casey Saenger, and Mike Miller for assistance in the field. We thank Stjepko Golubic (Boston University) for assistance during microscopy and with the identification of cyanobacteria. Special thanks to Mr. Rudi Rottenfusser, Carl Zeiss Inc. at Marine Biological Laboratory, Woods Hole, MA for providing support and advice in microscopy. The logistical support of Alla Skorokhod, Kim Anderson, John Bryden, Sue Fukada, and Chuck Corbitt was also greatly appreciated. Thanks to the Kiriritimati Ministers of the Environment and Fisheries for permission to conduct research on Christmas Island. The services of Bill Paupe, South Seas Air and the staff of the Captain Cook Hotel were also instrumental in the success of this research. We thank Anthony Faiia for the water  $\delta D$  analysis at Dartmouth College. We are grateful to Or-est Kawka and Valerie Schwab at the University of Washington for technical assistance and discussions. We would like to thank Alex L. Sessions and an anonymous reviewer as well as the Associate Editor Thomas S. Bianchi for their constructive comments on the original manuscript.

#### REFERENCES

- Agre P., Sasaki S. and Chrispeels M. J. (1993) Aquaporins—a family of water channel proteins. *Am. J. Physiol.* **265**(3), F461.
- Allakhverdiev S. I., Sakamoto A., Nishiyama Y., Inaba M. and Murata N. (2000a) Ionic and osmotic effects of NaCl-induced inactivation of photosystems I and II in *Synechococcus* sp. *Plant Physiol.* **123**(3), 1047–1056.
- Allakhverdiev S. I., Sakamoto A., Nishiyama Y. and Murata N. (2000b) Inactivation of photosystems I and II in response to osmotic stress in *Synechococcus*. Contribution of water channels. *Plant Physiol.* **122**(4), 1201–1208.
- Andersen N., Paul H. A., Bernasconi S. M., McKenzie J. A., Behrens A., Schaeffer P. and Albrecht P. (2001) Large and rapid climate variability during the Messinian salinity crisis: evidence from deuterium concentrations of individual biomarkers. *Geology* **29**(9), 799–802.
- Arp G., Thiel V., Reimer A., Michaelis W. and Reitner J. (1999) Biofilm exopolymers control microbialite formation at thermal springs discharging into the alkaline Pyramid Lake, Nevada, USA. *Sediment. Geol.* **126**(1–4), 159–176.
- Boursiac Y., Chen S., Luu D. T., Sorieul M., van den Dries N. and Maurel C. (2005) Early effects of salinity on water transport in Arabidopsis roots. Molecular and cellular features of aquaporin expression. *Plant Physiol.* **139**(2), 790–805.
- Burgoyne T. W. and Hayes J. M. (1998) Quantitative production of H-2 by pyrolysis of gas chromatographic effluents. *Anal. Chem.* **70**(24), 5136–5141.
- Castenholz R. W. (2001) General characteristics of the cyanobacteria. In *Bergey's Manual of Systematic Bacteriology*, Vol. 1 (eds. D. R. Boone and R. W. Castenholz). Springer, pp. 474–487.
- Chaykin S., Law J., Phillips A. H., Tchen T. T. and Bloch K. (1958) Phosphorylated intermediates in the synthesis of squalene. *Proc. Natl. Acad. Sci. USA* **44**(10), 998–1004.
- Chikaraishi Y. and Naraoka H. (2003) Compound-specific delta D-delta C-13 analyses of n-alkanes extracted from terrestrial and aquatic plants. *Phytochemistry* **63**(3), 361–371.
- Chikaraishi Y., Naraoka H. and Poulson S. R. (2004) Hydrogen and carbon isotopic fractionations of lipid biosynthesis among terrestrial (C3, C4 and CAM) and aquatic plants. *Phytochemistry* **65**(10), 1369–1381.
- Chrispeels M. J. and Agre P. (1994) Aquaporins—water channel proteins of plant and animal-cells. *Trends Biochem. Sci.* **19**(10), 421–425.
- Craig H. and Gordon L. (1965) Deuterium and oxygen 18 variations in the ocean and the marine atmosphere. In *Proceedings of a Conference on Stable Isotopes in Oceanographic Studies and Paleotemperatures* (ed. E. Tongiorni). CNR-Laboratorio di Geologia Nucleare, pp. 9–130.
- DeCoursey T.E. (2003). Voltage-gated proton channels and other proton transfer pathways (vol 83, pg 475, 2003). *Physiological Reviews* **83**(3), 1067–1067.
- Dembitsky V. M. and Srebnik M. (2002) Variability of hydrocarbon and fatty acid components in cultures of the filamentous cyanobacterium *Scytonema* sp isolated from microbial community “Black Cover” of limestone walls in Jerusalem. *Biochemistry (Moscow)* **67**(11), 1276–1282.
- Derosa M., Gambacor A., Minale L. and Bullock J. D. (1971) Bacterial triterpenes. *J. Chem. Soc. D Chem. Commun.* **12**, 619.
- Engelbrecht A. C. and Sachs J. P. (2005) Determination of sediment provenance at drift sites using hydrogen isotopes and unsaturation ratios in alkenones. *Geochim. Cosmochim. Acta* **69**(17), 4253–4265.
- Garcia-Pichel F., Kühl M., Nübel U. and Muyzer G. (1999) Salinity-dependent limitation of photosynthesis and oxygen exchange in microbial mats. *J. Phycol.* **35**(2), 227–238.

- Garcia-Pichel F., Nubel U. and Muyzer G. (1998) The phylogeny of unicellular, extremely halotolerant cyanobacteria. *Arch. Microbiol.* **169**(6), 469–482.
- Geitler L. (1932) Cyanophyceae. In Rabenhorst's Kryptogamenflora von Deutschland, Österreich und der Schweiz: 14 (1985 reprint: Königstein, Koletz Scientific Books) (ed. R. Kolkwitz). Akademische Verlagsgesellschaft.
- Gonfiantini R. (1986) Environmental isotopes in lake studies. In *Handbook of Environmental Isotope Geochemistry* (eds. P. Fritz and J. C. Fontes). Elsevier, pp. 113–168.
- Grimalt J. O., Dewit R., Teixidor P. and Albaiges J. (1992) Lipid biogeochemistry of *Phormidium* and *Microcoleus* mats. *Org. Geochem.* **19**(4–6), 509–530.
- Grossi V., Hirschler A., Raphael D., Rontani J. F., De Leeuw J. W. and Bertrand J. C. (1998) Biotransformation pathways of phytol in recent anoxic sediments. *Org. Geochem.* **29**(4), 845–861.
- Haines T. H. (1994) Water transport across biological-membranes. *FEBS Lett.* **346**(1), 115–122.
- Hilkert A. W., Douthitt C. B., Schlüter H. J. and Brand W. A. (1999) Isotope ratio monitoring gas chromatography/mass spectrometry of D/H by high temperature conversion isotope ratio mass spectrometry. *Rapid Commun. Mass Spectrom.* **13**, 1226–1230.
- Huang Y. S., Shuman B., Wang Y. and Webb T. (2004) Hydrogen isotope ratios of individual lipids in lake sediments as novel tracers of climatic and environmental change: a surface sediment test. *J. Paleolimnol.* **31**(3), 363–375.
- Ikan R., Baedeker M. J. and Kaplan I. R. (1975) Thermal alteration experiments on organic-matter in recent marine sediment. 2. Isoprenoids. *Geochim. Cosmochim. Acta* **39**(2), 187–194.
- Jahnke L. L., Enmbaye T., Hope J., Turk K. A., van Zuilen M., Des Marais D. J., Farmer J. D. and Summons R. E. (2004) Lipid biomarker and carbon isotopic signatures for stromatolite-forming, microbial mat communities and *Phormidium* cultures from Yellowstone National Park. *Geobiology* **2**, 31–47.
- Javor B. (1989) *Hypersaline Environments—Microbiology and Biogeochemistry*. Springer-Verlag.
- Kolattukudy P. E. (1967) Biosynthesis of paraffins in brassica oleracea—fatty acid elongation-decarboxylation as a plausible pathway. *Phytochemistry* **6**(7), 963–975.
- Kolattukudy P. E. (1981) Structure, biosynthesis, and biodegradation of cutin and suberin. *Ann. Rev. Plant Physiol. Plant Mol. Biol.* **32**, 539–567.
- Komárek J. and Anagnostidis K. (1999) Cyanoprokaryota, 1. Teil: chroococcales. In *Süßwasserflora von Mitteleuropa*, Vol. 19/1 (eds. H. Ettl, G. Gärtner, H. Heynig and D. Mollenhauer). Gustav Fischer Verlag, pp. 1–548.
- Komárek J. and Anagnostidis K. (2005) Cyanoprokaryota, 2. Teil: oscillatoriales. In *Süßwasserflora von Mitteleuropa* (eds. B. Bündel, G. Gärtner, L. Krientitz and M. Schlager). Gustav Fischer Verlag, pp. 1–759.
- Kreuzer-Martin H. W., Lott M. J., Ehleringer J. R. and Hegg E. L. (2006) Metabolic processes account for the majority of the intracellular water in log-phase *Escherichia coli* cells as revealed by hydrogen isotopes. *Biochemistry* **45**(45), 13622–13630.
- Lange B., Rujan T., Martin W. and Croteau R. (2000) Isoprenoid biosynthesis: the evolution of two ancient and distinct pathways across genomes. *Proc. Natl. Acad. Sci. USA* **97**(24), 13172–13177.
- Lichtenthaler H. (2004) The 1-deoxy-D-xylulose-5-phosphate pathway of isoprenoid biosynthesis in plants. *Annu. Rev. Plant Physiol. Plant Mol. Biol.* **50**, 47–65.
- Lochte K. and Turley C. M. (1988) Bacteria and cyanobacteria associated with phytodetritus in the deep-sea. *Nature* **333**(6168), 67–69.
- Lynen F., Eggerer H., Henning U. and Kessel I. (1958) Farnesylpyrophosphat und 3-methyl-delta-3-butenyl-1-pyrophosphat, die biologischen vorstufen des squalens zur biosynthese der terpene.3. *Angew. Chem. Int. Ed.* **70**(24), 738–742.
- Moezelaar R. and Stal L. J. (1997) A comparison of fermentation in the cyanobacterium *Microcystis* PCC7806 grown under a light/dark cycle and continuous light. *Eur. J. Phycol.* **32**(4), 373–378.
- Nübel U., Garcia-Pichel F., Clavero E. and Muyzer G. (2000) Matching molecular diversity and ecophysiology of benthic cyanobacteria and diatoms in communities along a salinity gradient. *Environ. Microbiol.* **2**(2), 217–226.
- Pagani M., Pedentchouk N., Huber M., Sluijs A., Schouten S., Brinkhuis H., Damste J. S. S., Dickens G. R. and Scientists E. (2006) Arctic hydrology during global warming at the Palaeocene/Eocene thermal maximum. *Nature* **442**(7103), 671–675.
- Pahnke K., Sachs J. P., Keigwin L. D., Timmermann A. and Xie S.-P. (2007) Eastern tropical Pacific hydrologic changes during the past 27,000 years from D/H ratios in alkenones. *Paleoceanography*, in press.
- Pancost R. D., Pressley S., Coleman J. M., Benning L. G. and Mountain B. W. (2005) Lipid biomolecules in silica sinters: indicators of microbial biodiversity. *Environ. Microbiol.* **7**(1), 66–77.
- Pomati F., Burns B. and Neilan B. (2004) Use of ion-channel modulating agents to study cyanobacterial Na(+)-K(+) fluxes. *Biol. Proc. Online* **6**, 137–143.
- Prahl F. G., Hayes J. M. and Xie T. M. (1992) Diploptene—an indicator of terrigenous organic-carbon in Washington Coastal sediments. *Limnol. Oceanogr.* **37**(6), 1290–1300.
- Rohmer M., Bouvierne P. and Ourisson G. (1984) Distribution of Hopanoid Triterpenes in Prokaryotes. *J. Gen. Microbiol.* **130**(MAY), 1137–1150.
- Rohmer M., Knani M., Simonin P., Sutter B. and Sahn H. (1993) Isoprenoid biosynthesis in bacteria—a novel pathway for the early steps leading to isopentenyl diphosphate. *Biochem. J.* **295**, 517–524.
- Sachse D., Radke J. and Gleixner G. (2004) Hydrogen isotope ratios of recent lacustrine sedimentary *n*-alkanes record modern climate variability. *Geochim. Cosmochim. Acta* **68**(23), 4877–4889.
- Sachse D., Radke J. and Gleixner G. (2006) Delta D values of individual *n*-alkanes from terrestrial plants along a climatic gradient—implications for the sedimentary biomarker record. *Org. Geochem.* **37**(4), 469–483.
- Saenger C., Miller M., Smittenberg R. H. and Sachs J. P. (2006) A physico-chemical survey of inland lakes and saline ponds: Christmas Island (Kiritimati) and Washington (Teraina) Islands, Republic of Kiribati. *Saline Syst.* **2**(8).
- Sakata S., Hayes John M., McTaggart A. R., Evans R. A., Leckrone K. J. and Togaski R. K. (1997) Carbon isotopic fractionation associated with lipid biosynthesis by a cyanobacterium: relevance for interpretation of biomarker records. *Geochim. Cosmochim. Acta* **61**(24), 5379–5389.
- Sauer P. E., Eglinton T. I., Hayes J. M., Schimmelman A. and Sessions A. L. (2001) Compound-specific D/H ratios of lipid biomarkers from sediments as a proxy for environmental and climatic conditions. *Geochim. Cosmochim. Acta* **65**(2), 213–222.
- Schefuss E., Schouten S. and Schneider R. R. (2005) Climatic controls on central African hydrology during the past 20,000 years. *Nature* **437**(7061), 1003–1006.
- Schmidt H. L., Werner R. A. and Eisenreich W. (2003) Systematics of 2H patterns in natural compounds and its importance for the elucidation of biosynthetic pathways. *Phytochem. Rev.* **2**, 61–85.
- Schouten S., Ossebaer J., Schreiber K., Kienhuis M. V. M., Langer G., Benthien A. and Bijma J. (2006) The effect of temperature,

- salinity and growth rate on the stable hydrogen isotopic composition of long chain alkenones produced by *Emiliania huxleyi* and *Gephyrocapsa oceanica*. *Biogeosciences* **3**(1), 113–119.
- Schwender J., Seemann M., Lichtenthaler H. K. and Rohmer M. (1996) Biosynthesis of isoprenoids (carotenoids, sterols, prenyl side-chains of chlorophylls and plastoquinone) via a novel pyruvate/glyceraldehyde 3-phosphate non-mevalonate pathway in the green alga *Scenedesmus obliquus*. *Biochem. J.* **316**, 73–80.
- Sessions A. L., Burgoyne T. W. and Hayes J. M. (2001) Determination of the H-3 factor in hydrogen isotope ratio monitoring mass spectrometry. *Anal. Chem.* **73**(2), 200–207.
- Sessions A. L., Burgoyne T. W., Schimmelmann A. and Hayes J. M. (1999) Fractionation of hydrogen isotopes in lipid biosynthesis. *Org. Geochem.* **30**(9), 1193–1200.
- Sessions A. L. and Hayes J. M. (2005) Calculation of hydrogen isotopic fractionations in biogeochemical systems. *Geochim. Cosmochim. Acta* **69**(3), 593–597.
- Shiea J., Brassell S. C. and Ward D. M. (1991) Comparative-analysis of extractable lipids in hot-spring microbial mats and their component photosynthetic bacteria. *Org. Geochem.* **17**(3), 309–319.
- Simoneit B. R. T., Summons R. E. and Jahnke L. L. (1998) Biomarkers as tracers for life on early Earth and Mars. *Orig. Life Evol. Biosphere* **28**(4-6), 475–483.
- Smith F. A. and Freeman K. H. (2006) Influence of physiology and climate on delta D of leaf wax *n*-alkanes from C-3 and C-4 grasses. *Geochim. Cosmochim. Acta* **70**(5), 1172–1187.
- Stal L. J. (1995) Physiological ecology of cyanobacteria in microbial mats and other communities. *New Phytolog.* **131**(1), 1–32.
- Tanghe A., Van Dijck P. and Thevelein J. M. (2006) Why do microorganisms have aquaporins? *Trends Microbiol.* **14**(2), 78–85.
- Trichet J., Defarge C., Tribble J., Tribble G. and Sansone F. (2001) Christmas Island lagoonal lakes, models for the deposition of carbonate-evaporite-organic laminated sediments. *Sediment. Geol.* **140**(1-2), 177–189.
- Valencia M. (1977) Christmas Island (Pacific Ocean): reconnaissance geologic observations. *Atoll Res. Bull.* **197**, 1–17.
- Waditee R., Hibino T., Tanaka Y., Nakamura T., Incharoensakdi A. and Takabe T. (2001) Halotolerant cyanobacterium *Aphanotece halophytica* contains an Na(+)/H(+) antiporter, homologous to eukaryotic ones, with novel ion specificity affected by C-terminal tail. *J. Biol. Chem.* **276**(40), 36931–36938.
- Werner R. A. and Brand W. A. (2001) Referencing strategies and techniques in stable isotope ratio analysis. *Rapid Commun. Mass Spectrom.* **15**(7), 501–519.
- Xu X. Q., Beardall J. and Hallam N. D. (1998) Modification of fatty acid composition in halophilic Antarctic microalgae. *Phytochemistry* **49**(5), 1249–1252.
- Zhang Z. and Sachs J. (2007) Hydrogen isotope fractionation in freshwater algae: I. Variations among lipids and species. *Org. Geochem.* **38**, 532–608.

Associate editor: Tom Bianchi